© 2018. Published by The Company of Biologists Ltd | Development (2018) 145, dev159012. doi:10.1242/dev.159012

RESEARCH ARTICLE

A non-autonomous function of the core PCP protein VANGL2 directs peripheral axon turning in the developing cochlea

Satish R. Ghimire[1], Evan M. Ratzan[2] and Michael R. Deans[1,2,3,*]

ABSTRACT

The cochlea is innervated by neurons that relay sound information from hair cells to central auditory targets. A subset of these are the type II spiral ganglion neurons, which have nociceptive features and contribute to feedback circuits providing neuroprotection in extreme noise. Type II neurons make a distinctive 90° turn towards the cochlear base to synapse with 10-15 outer hair cells. We demonstrate that this axon turning event requires planar cell polarity (PCP) signaling and is disrupted in *Vangl2* and *Celsr1* knockout mice, and that VANGL2 acts non-autonomously from the cochlea to direct turning. Moreover, VANGL2 is asymmetrically distributed at intercellular junctions between cochlear supporting cells, and in a pattern that could allow it to act directly as an axon guidance cue. Together, these data reveal a non-autonomous function for PCP signaling during axon guidance occurring in the tissue that is innervated, rather than the navigating growth cone.

KEY WORDS: Cochlea, Planar cell polarity, Vangl2, Axon guidance, Spiral ganglion neuron

INTRODUCTION

Auditory hair cells of the mammalian cochlea are innervated by the bipolar neurons of the spiral ganglion, which relay auditory information through the VIIIth cranial nerve. Spiral ganglion neurons (SGNs) are afferent sensory neurons distributed between two functional subtypes. The type I SGNs are the most common (90-95%); they innervate inner hair cells (IHCs) and convey the salient features of sound. In contrast, the remaining type II SGNs are thought to serve important neuroprotective rather than sensory functions, likely by acting as auditory nociceptors (Flores et al., 2015; Liu et al., 2015; Maison et al., 2016), although an alternative contribution to feedback circuitry controlling auditory sensitivity has also been proposed (Froud et al., 2015). Type II SGNs innervate all three rows of outer hair cells (OHCs), with each fiber receiving information from 10-15 OHCs (Berglund and Ryugo, 1987; Raphael and Altschuler, 2003). In addition to integrating subthreshold glutamatergic inputs from this complement of OHCs, type II SGNs may also respond to ATP released upon trauma (Weisz et al., 2009). In contrast, the more numerous type I SGNs make one-to-one contacts with IHCs and an individual IHC may be contacted by 15-20 type I SGN peripheral axons. Although the peripheral processes of spiral ganglion neurons are post-synaptic to hair cells, they are frequently referred to as peripheral axons because they conduct action potentials and, in the case of type I SGNs, are also myelinated (Weisz et al., 2009; Nayagam et al., 2011).

The integration of OHC inputs is facilitated by the unique morphology of type II SGNs, which is an additional characteristic that distinguishes them from their type I counterparts. Whereas the radial projection of type I fibers terminates at a synapse onto the IHCs, the type II fibers extend beyond the IHCs before making a distinctive 90° turn towards the cochlear base (Berglund and Ryugo, 1987). After turning, a type II fiber will extend beneath a row of OHCs, forming synapses with multiple cells along the way while contributing to one of three fiber tracts known as the outer spiral bundles. A striking feature of type II SGNs is that their peripheral axons always project towards the cochlear base, which resembles the commissural axons of the neural tube that also make a similar 90° turn (Bovolenta and Dodd, 1990; Lyuksyutova et al., 2003). Type II SGN growth cone turning begins at embryonic day 16.5 (E16.5) in locations near the cochlear base and progresses sequentially along the length of the cochlear spiral towards the apex until birth (Koundakjian et al., 2007). Despite the remarkable fidelity of growth cone trajectories preceding the appearance of this stereotyped neuronal anatomy, the molecular mechanisms underlying this distinctive pathfinding event are not understood.

Typically, during axon guidance, navigating growth cones interpret guidance cues in the environment through cell-surface receptors that initiate cell-signaling cascades and dynamic changes in the cytoskeleton (Bashaw and Klein, 2010; O'Donnell et al., 2009). The role of classic axon guidance cues, including semaphorin, ephrin, slit and netrin, and the neurotrophic factors neurotrophin 3 and brain-derived neurotrophic factor have been studied extensively during SGN development and patterning in the mouse (Coate et al., 2015; Defourny et al., 2013; Fritzsch et al., 1997a,b; Kim et al., 2016; Wang et al., 2013). Although these molecules make important contributions to SGN survival and migration, and towards the patterning of type I SGNs, type II SGN axon turning is not altered when the genes encoding these proteins are mutated. The distinct anterior turn of commissural axons also does not require classic axon guidance cues and instead is guided by non-canonical Wnt signaling and the core planar cell polarity (PCP) proteins VANGL2, FZD3 and CELSR3 (Lyuksyutova et al., 2003; Onishi et al., 2013; Shafer et al., 2011). Core PCP proteins also regulate subcortical axon tract formation (Feng et al., 2016; Qu et al., 2014), anteroposterior growth cone guidance of dopaminergic and serotonergic neurons in the brainstem (Fenstermaker et al., 2010; Tissir et al., 2005; Wang et al., 2002), and the caudal migration of facial branchiomotor neurons (FBMN) in mice and zebrafish (Glasco et al., 2012; Jessen et al., 2002; Wada et al., 2006; Walsh et al., 2011). Thus, core PCP proteins are emerging as

[1]Department of Neurobiology and Anatomy, University of Utah School of Medicine, Salt Lake City, UT 84112, USA. [2]Interdepartmental Program in Neuroscience, University of Utah School of Medicine, Salt Lake City, UT 84112, USA. [3]Department of Surgery, Division of Otolaryngology, University of Utah School of Medicine, Salt Lake City, UT 84132, USA.

*Author for correspondence (michael.deans@utah.edu)

M.R.D., 0000-0001-6319-7945

Received 30 August 2017; Accepted 14 May 2018

Development (2018) 145, dev159012. doi:10.1242/dev.159012

important regulators of cellular polarization in a variety of dynamic developmental events (Davey and Moens, 2017).

The role of PCP signaling in development of the mammalian ear is well established, particularly for the sensory receptor hair cells where core PCP proteins are required to coordinate the orientation of polarized stereociliary bundles between neighboring cells (Copley et al., 2013; Curtin et al., 2003; Duncan et al., 2017; Montcouquiol et al., 2003; Stoller et al., 2018; Wang et al., 2006a; Yin et al., 2012). Given the striking morphological similarities between commissural neurons and type II SGNs, and the role of PCP signaling in both commissural axon guidance and inner ear development, we hypothesized that PCP could similarly direct type II SGN development. Consistent with this premise, we demonstrate that type II fiber turning is randomized in *Vangl2* KOs and turning errors are frequent in several other core PCP mutants. In contrast, we demonstrate that *Vangl2* is not required in the type II SGN to direct turning and instead acts non-autonomously within the organ of Corti of the cochlea to steer the growth of type II fibers towards the cochlear base. Moreover, VANGL2 is strategically located at the basolateral surfaces of the inner pillar cells (IPCs) where type II fiber turning is first evident. We propose that during cochlear innervation, VANGL2 functions as a guidance cue in the organ of Corti that directs axon pathfinding, rather than as a cell-autonomous effector within the navigating growth cone.

RESULTS

Type II SGN peripheral axons make stereotyped turns towards the cochlear base

Type II SGN peripheral axons have a unique morphology characterized by a 90° turn towards the cochlear base occurring after the initial radial projection extends beyond the IHCs and passes between the IPCs (Appler and Goodrich, 2011; Berglund and Ryugo, 1987). In the developing cochlea, the distal extensions of turning fibers can be seen through NF200 immunolabeling of whole-mount preparations (Fig. 1A-D). Similar to other aspects of cochlear development, type II SGN maturation occurs along a gradient from the basal to apical turn, and type II fiber turning is first evident in the base at E17.5, with fasciculation into three outer spiral bundles in this location at E18.5 (Fig. 1C,D). An outer spiral bundle can be visualized beneath each of the three OHC rows, along the neural side of a population of supporting cells called Deiters cells. Although NF200 is not specific to the type II fibers, at these stages efferent neurons have not reached the OHCs (Huang et al., 2007) and the majority of afferent neurons projecting beyond the IHCs are thought to be type II (Druckenbrod and Goodrich, 2015). More significantly, all NF200-positive fibers extending beyond the IHCs turn towards the cochlear base. Although peripherin may be a more specific marker for type II SGNs at later stages, NF200 generally provides a reliable readout of neuronal morphology during these earlier stages of development.

Auditory hair cells are isolated from each other by intervening populations of supporting cells that contribute to the biophysical properties of the cochlea. Hair cells and supporting cells are organized in a pseudostratified epithelium, with hair cells located in more apical positions than supporting cells, as seen in cochlear cross sections (Fig. 1E,F). Different classes of supporting cells can be distinguished based upon morphological characteristics and position along the neural:abneural axis of the cochlea (Fig. 1C-F). IPCs and outer pillar cells (OPCs) separate IHCs from the first row of OHCs, whereas Deiters cells surround the remaining OHCs. IPCs are further distinguished by their distinctive cuboidal nuclear morphology (Fig. 1C,D). While projecting towards the cochlear base, NF200-positive fibers pass between neighboring IPCs and then dive deeper into the tissue, passing beneath the OPCs and Deiters cells, before turning and ascending towards the OHCs in the outer spiral bundles (Fig. 1E,F). As a result, the spiral bundles are located in a more superficial plane than radially projecting and turning type II SGN fibers. Although axonal turning is first evident as the fibers emerge from between the IPCs, additional turning events can occur as some fibers traverse between the IPCs and the outermost spiral bundle.

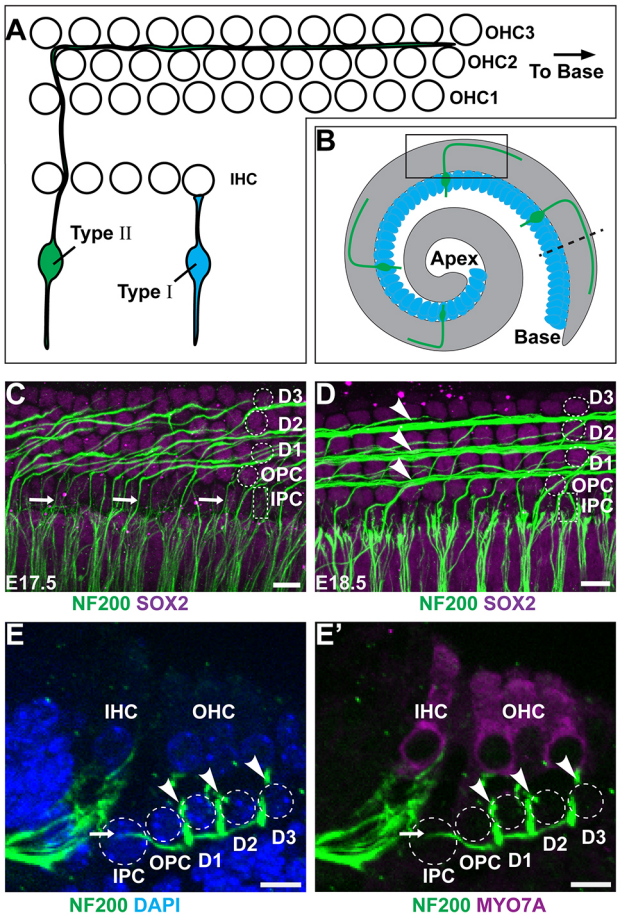

Fig. 1. Type II SGN peripheral axons have a stereotyped pattern of cochlear innervation. (A) The type II SGN peripheral axon turns towards the cochlear base and forms *en passant* synapses with numerous outer hair cells (OHCs), whereas the type I SGNs make exclusive one-to-one contact with inner hair cells (IHCs). (B) A schematic representation of the cochlea showing type II neurons projecting towards the cochlear base. The boxed region indicates the orientation of whole-mount immunolabeling in C,D. The dashed line indicates the orientation of cochlear cross sections in E,F. (C) At E17.5 in the cochlear base type II SGN fibers (arrows) pass between inner pillar cells (IPCs) before turning in front of outer pillar cells (OPCs) or subsequent rows of Deiters cells (D1, D2, D3). Supporting cell nuclei are selectively labeled for SOX2. (D) At E18.5, a more mature type II innervation pattern has formed with the three rows of outer spiral bundles (arrowheads) located in front of each row of Deiters cells. (E,E′) A cross-section of the P0 cochlea demonstrates type II SGN processes (arrow) passing between IPC nuclei before diving beneath the OPCs and returning superficially (arrowheads) to contact MYO7A-expressing hair cells. Supporting cell types are outlined in C-E′. Scale bars: 10 µm.

Type II SGN turning towards the cochlear base requires core PCP proteins

Core PCP proteins are important for inner ear development and direct the polarized organization of auditory and vestibular hair cell stereociliary bundles (Curtin et al., 2003; Montcouquiol et al., 2003;

Development (2018) 145, dev159012. doi:10.1242/dev.159012

Wang et al., 2006b; Yin et al., 2012). Core PCP proteins also guide axon pathfinding events that underlie the anterior turning of commissural fibers in the spinal cord (Lyuksyutova et al., 2003; Onishi et al., 2013; Shafer et al., 2011), subcortical axon tract formation (Tissir et al., 2005; Wang et al., 2002), and anteroposterior growth cone guidance of dopaminergic and serotonergic neurons in the brainstem (Fenstermaker et al., 2010). These observations suggest that PCP signaling may similarly guide type II fiber turning in the cochlea. Consistent with this hypothesis, *Vangl2* and *Fzd3* mRNAs are present throughout the organ of Corti of the cochlea and in the SGN (Fig. 2A-D). *Celsr1* and *Celsr3* are similarly expressed in the SGN, and are found in overlapping patterns in the organ of Corti, with *Celsr1* mRNA throughout and *Celsr3* mRNA restricted to a region adjacent to the hair cells [Fig. 2E,F and Shima et al. (2002)]. Consistent with this expression, CELSR1, FZD3 and VANGL2 proteins are enriched at boundaries between hair cells and supporting cells throughout the organ of Corti (Curtin et al., 2003; Duncan et al., 2017; Montcouquiol et al., 2006; Wang et al., 2006b), and mutations in *Celsr1*, *Fzd3* and *Vangl2* result in mis-oriented stereociliary bundles (Curtin et al., 2003; Montcouquiol et al., 2003; Wang et al., 2006b).

The contribution of core PCP signaling to type II SGN turning was evaluated in *Vangl2* KO mice by immunolabeling type II fibers with NF200 at E18.5. Although *Vangl2* KOs do not survive beyond birth because of neural tube defects (Yin et al., 2012), the type II fibers have already initiated turning at this late embryonic stage (Koundakjian et al., 2007). In littermate controls, NF200-positive type II fibers in the basal turn extend beyond the termination of type I fibers and turn towards the cochlear base, forming three outer spiral bundles (Fig. 3A). In apical locations, individual NF200-labeled axonal endings can be resolved projecting towards the cochlear base (Fig. 3B), and individual fibers can be resolved by focal DiI labeling (Fig. 3C). In contrast, in the basal and apical turns of the *Vangl2* KO cochlea, many NF200-positive fibers turn incorrectly towards the cochlear apex (Fig. 3D,E), and individual turning errors are similarly resolved using DiI (Fig. 3F). As core PCP mutants do not survive beyond birth, and because of the immature organization of NF200-positive fibers in the middle and apical turns of the cochlea at this stage, phenotypes were quantified only in the base. When quantified, the average frequency of turning errors in *Vangl2* KOs is 50%, suggesting that turning may be randomized in the absence of PCP signaling; however, this frequency varied between individual animals (Fig. 3I).

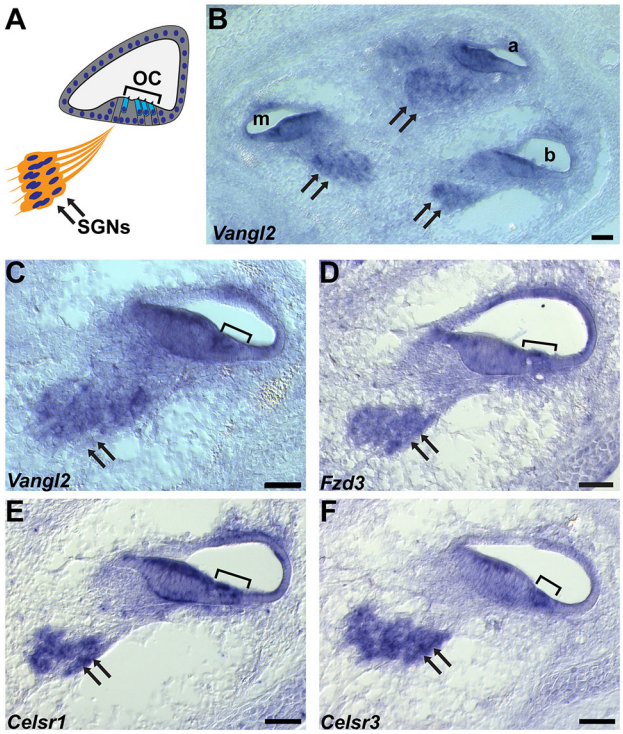

Fig. 2. Core PCP gene expression in the mouse cochlea. (A) A schematic representation of a cochlear cross-section showing the location of the SGN (arrows), organ of Corti (OC) and hair cells (bracket). (B-F) *In-situ* hybridizations of the E16.5 cochlea show *Vangl2* (B,C), *Fzd3* (D), *Celsr1* (E) and *Celsr3* (F) gene expression in the SGN and cochlea. a, apical; m, middle; b, basal turns of the cochlear duct. Scale bars: 50 µm.

In addition to VANGL2, the core PCP proteins FZD3 and CELSR3 have well documented roles in axon pathfinding in the mouse brain and spinal cord (Lyuksyutova et al., 2003; Onishi et al., 2013; Shafer et al., 2011; Tissir et al., 2005; Wang et al., 2002). Consistent with this, there is a partially penetrant yet statistically significant type II fiber turning defect in the basal turn of the *Fzd3* KO cochlea (Fig. 3G,I). In notable contrast, despite CELSR3 functions in CNS development (Tissir et al., 2005; Zhou et al., 2009) and *Celsr3* expression in the SGN (Fig. 2F), *Celsr3* KO mice have normal type II fiber turning at E18.5 that is comparable with littermate controls (Fig. 3I). Instead, turning errors are prominent in *Celsr1* KOs, with ∼30% of type II fibers turning incorrectly towards the cochlear apex at postnatal day 0 (P0) (Fig. 3H,I). Although the absence of turning errors in *Celsr3* KOs may be because of compensation by *Celsr2*, the frequency of turning errors in *Celsr1* KO mice is remarkable considering that *Celrs1* principally regulates epithelia PCP and not axon pathfinding (Goffinet and Tissir, 2017), and suggests PCP signaling within the organ of Corti may indirectly contribute to growth cone turning.

To determine whether type II SGN turning is impacted throughout the length of the cochlea and whether mis-turned fibers are maintained at hearing onset, viable *Vangl2* CKOs were generated using *Pax2*-Cre (Copley et al., 2013). In this line, Cre-mediated recombination occurs throughout the cochlear duct and neurons of the SGN (Fig. 4A) (Ohyama and Groves, 2004). In *Pax2*-Cre; *Vangl2* CKOs, 34% of type II fibers turned incorrectly towards the cochlear apex (Fig. 4B-D) and turning errors occurred with comparable frequency along the length of the cochlea (Fig. 4E). A similar frequency was measured when individual type II fibers were labeled with DiI rather than with NF200 (Fig. 4D). The reduced penetrance of the mutant phenotype in *Pax2*-Cre; *Vangl2* CKOs compared with *Vangl2* KOs is not because of compensation by *Vangl1*, which acts redundantly with *Vangl2* to coordinate stereociliary bundle polarity (Song et al., 2010; Torban et al., 2008), because there is no turning phenotype in *Vangl1* KOs and the phenotype is not enhanced in *Pax2*-Cre; *Vangl1*; *Vangl2* dCKOs (Fig. 4D). Although it is possible that VANGL2 protein that perdures beyond Cre-mediated gene deletion could guide turning of some fibers in CKOs, these results demonstrate that type II SGN turning is regulated by *Vangl2* and not *Vangl1*, and that the *Vangl2* CKO line can be used to establish the site of *Vangl2* function.

During neural development, the establishment of functional circuitry involves the pruning and retraction of inappropriate or excessive connections made by individual neurons (Riccomagno and Kolodkin, 2015). In the cochlea, type II SGNs are generated in excess and subsequently culled through a wave of apoptosis (Barclay et al., 2011). Thus, ∼25% of SGNs are lost during the first postnatal week, mainly through the selective elimination of type II

Development (2018) 145, dev159012. doi:10.1242/dev.159012

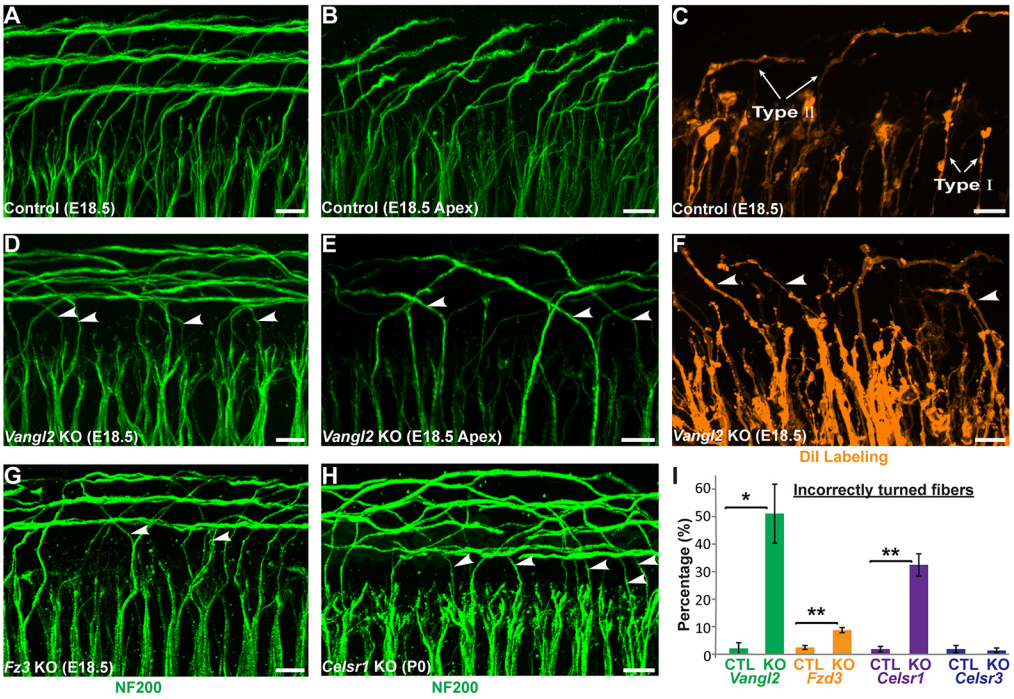

Fig. 3. Normal turning of type II peripheral axons is disrupted in PCP mutants. (A,B) Whole-mount NF200 immunolabeling of the type II peripheral axons reveals stereotyped turns towards the cochlear base in the more mature basal (A) and less mature apical (B) regions of the E18.5 mouse cochlea. (C) The morphology of individual type I and type II neurons is also revealed by sparse DiI labeling. (D-F) In the *Vangl2* KO cochlea, incorrectly turned axons (arrowheads) projecting towards the cochlear apex can be identified using both NF200 (D,E) and DiI (F). Similar turning errors occur in the basal region of *Fzd3* KOs (G) at E18.5 and in *Celsr1* KOs (H) at P0. (I) Quantification of averaged turning error frequencies in *Vangl2* (n=3), *Fzd3* (n=3), *Celsr1* (n=3) and *Celsr3* (n=3) KO mice relative to littermate controls (n=3 for each). Data are mean±s.e.m. *P<0.05, **P<0.01 for KOs versus littermate controls (Student's t-test). Scale bars: 10 µm.

SGNs (Barclay et al., 2011). To test the potential for incorrectly turned fibers to be eliminated by apoptosis, type II fibers were analyzed in *Pax2*-Cre; *Vangl2* CKOs at P10, a developmental stage that is after apoptotic pruning and immediately before the onset of hearing. Despite a reduction in the number of NF200-positive fibers contributing to the outer spiral bundles, incorrectly turned processes extending towards the cochlear apex persisted in the *Pax2*-Cre; *Vangl2* CKO cochlea (Fig. 4F,G).

Vangl2 functions non-autonomously to direct type II SGN turning

The similarities between type II SGN phenotypes in *Vangl2* KOs and commissural axon phenotypes in PCP mutants suggest that VANGL2 may function in the peripheral axon growth cone to promote turning towards the cochlear base. However, type II SGN turning errors are frequent in mice in which *Celsr1*, a gene that has only been associated with epithelial PCP, has been knocked out (Fig. 3H); by contrast, mice in which *Celsr3*, a gene that regulates axon pathfinding in other contexts (Goffinet and Tissir, 2017; Onishi et al., 2013; Tissir et al., 2005), has been knocked out do not exhibit such turning errors (Fig. 3I). Moreover, as *Vangl2* figures prominently in the development of planar polarity in the cochlear duct (Copley et al., 2013; Montcouquiol et al., 2003; Yin et al., 2012), it is possible that VANGL2 acts non-autonomously from the duct to guide axon turning. Consistent with this possibility, *Vangl2* functions non-autonomously in the zebrafish hindbrain to direct FBMN migration through dynamic processes that are analogous to growth cone migration (Davey et al., 2016; Jessen et al., 2002; Walsh et al., 2011; Sittaramane et al., 2013).

To distinguish between alternative sites of *Vangl2* function in the peripheral axon versus the organ of Corti, SGN-specific *Vangl2* CKOs were generated using *Bhlhb5*-Cre transgenic mice in which gene deletion has been documented at E9.5 (Appler et al., 2013). Consistent with this, *Bhlhb5*-Cre-mediated reporter activation occurs in type I and type II neurons (Fig. 5A), and occurs at E13.5, prior to cochlear innervation (Fig. 5B). In addition *Vangl2* mRNA is dramatically reduced in the SGN before type II axon turning at E16.5 in *Bhlhb5*-Cre; *Vangl2* CKOs (Fig. 5D,E). However, when compared with littermate controls at P2, no significant turning errors were detected in *Bhlhb5*-Cre; *Vangl2* CKOs (Fig. 5F-I), demonstrating that VANGL2 is not required in type II SGNs to mediate turning. In a complementary experiment, peripheral axon turning was evaluated following neuronal deletion using *Pou4f2*-Cre and, similarly, no significant turning errors were detected (data not shown).

The contribution of cochlear VANGL2 was evaluated using *Emx2*^{Cre} knock-in mice (Ono et al., 2014) that have robust Cre activity throughout the cochlear duct (Fig. 6A). *Emx2*-Cre is also active in some cells of the SGN; however, these occur in a gradient along the length of the cochlea, and are more frequent in the apical turn and less in the base (Fig. 6B). Moreover, *Emx2*-Cre reduces *Vangl2* mRNA from a region of the cochlea corresponding to the organ of Corti (Fig. 6D,E). When quantified, 26% of type II fibers turn incorrectly in *Emx2*-Cre; *Vangl2* CKO cochleas (Fig. 6F-H), and turning errors occur with comparable frequency in apical and basal turns (Fig. 6H), demonstrating that VANGL2 acts non-autonomously and is not required in the peripheral axon. The site of *Vangl2* gene deletion was further restricted using *Fgfr3*-iCre^{ER}, which is activated in IPCs, OPCs and Deiters cells following daily tamoxifen administration from E14.5 to E16.5 [Fig. 6I,J and Anttonen et al. (2012)]. When *Vangl2* is selectively eliminated from supporting cells in *Fgfr3*-iCre^{ER}; *Vangl2* CKOs, incorrectly turned type II peripheral axons are prevalent in the middle and apical turns, where they can be visualized projecting towards the cochlear apex (Fig. 6L). When quantified, 27% of type II fibers turned incorrectly in the middle turn of the CKO cochlea (Fig. 6M). The absence of turning errors in the basal turn is likely because of VANGL2 expression before Cre^{ER} activation. Altogether, these genetic dissections of *Vangl2* are consistent with a non-autonomous function of VANGL2 in the organ of Corti that directs peripheral axon turning.

VANGL2 is asymmetrically distributed in supporting cells of the organ of Corti

The mechanism by which *Vangl2* could direct axon turning is dependent upon the subcellular distribution of VANGL2 protein

Development (2018) 145, dev159012. doi:10.1242/dev.159012

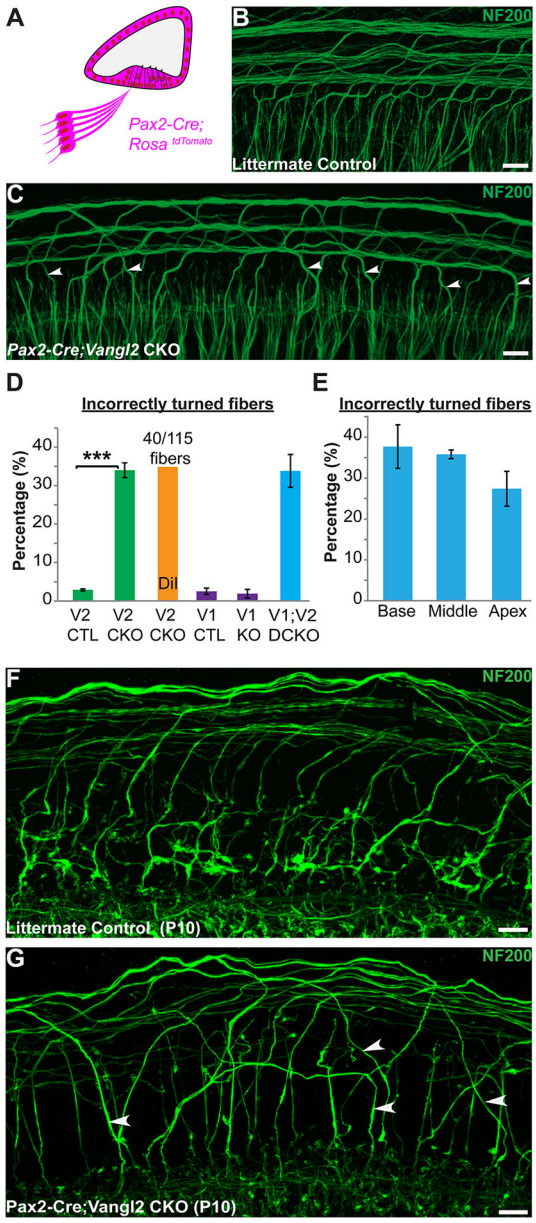

Fig. 4. Incorrectly turned type II fibers are maintained during postnatal development. (A) Schematic representation of *Pax2*-Cre-mediated recombination in the mouse cochlea. (B,C) Whole-mount NF200 immunolabeling of type II peripheral axons at P2 illustrates incorrectly turned processes (arrowheads) extending towards the cochlear apex in *Pax2-Cre; Vangl2* CKOs (C) that are not found in littermate controls (B). (D) Quantification of average turning error frequency of NF200-labeled axons in *Vangl2* CKO (n=4), *Vangl1* KO (n=3) and *Vangl1/2* CKO (n=3) mice relative to littermate controls (n=3). As a technical validation, the frequency of turning errors for individual *Pax2*-Cre; *Vangl2* CKO neurons labeled with DiI is also included. Turning errors were not detected in *Vangl1* KOs and penetrance of the *Vangl2* CKO phenotype was not enhanced with the loss of *Vangl1* (P=0.97 compared with *Pax2*-Cre;*Vangl2* CKOs using Student's *t*-test). Data are mean±s.e.m. Asterisks show significant differences between genotypes using Student's *t*-test (***P<0.001). (E) No differences in the frequency of turning errors were detected along the length of the *Pax2*-Cre; *Vangl2* CKO cochlea at P2 (P=0.21 using one-way ANOVA). (F,G) Type II peripheral axon turning errors persist in *Pax2*-Cre; *Vangl2* CKOs at P10 (arrowheads). Scale bars: 10 µm.

within the organ of Corti. Previous studies have shown VANGL2 enriched at apical cell boundaries between hair cells and supporting cells (Montcouquiol et al., 2006), where VANGL2 coordinates the orientation of stereociliary bundles between neighboring hair cells. However, it is unlikely that hair cell planar polarity contributes to type II fiber turning because OHC1 and OHC2 stereociliary bundle orientation is not altered in *Vangl2* KOs (Yin et al., 2012), yet type II fiber turning is random in the vicinity of OHC1 in the absence of *Vangl2* (Fig. 3D,E). Similarly, turning errors are frequent in *Celsr1* KOs (Fig. 3H) despite the lack of a hair cell PCP phenotype in the KO cochlea (Duncan et al., 2017), further indicating that type II SGN turning is not influenced by hair cell planar polarity.

Hair cells and supporting cells are organized within a pseudostratified epithelium in which the hair cells are located in an apical position relative to the underlying supporting cells (Fig. 7A). Although there are multiple classes of supporting cells with differing morphologies, each extends an apical process to the surface of the organ of Corti that separates hair cells from each other. Whole-mount immunolabeling demonstrates a polarized distribution of VANGL2 at OHCs to supporting cell boundaries oriented perpendicular to the neural:abneural axis (Fig. 7B). VANGL2 is also present at the basolateral surfaces of supporting cells where they contact each other directly without an intervening hair cell (Fig. 7C,C′). This is evident by colocalization with the basolateral marker E-cadherin (Fig. 7E,F) and labeling of adjacent OPCs by CD44 (Fig. 7G,H) (Hertzano et al., 2010). In this location, VANGL2 is enriched at cell boundaries parallel to the neural: abneural axis of the cochlea. This is similar to the distribution of the core PCP protein PRICKLE2 outside of the organ of Corti in greater epithelial ridge cells (Copley et al., 2013; Goodyear et al., 2017). CELSR1 has a similar distribution to VANGL2 at apical (Duncan et al., 2017) and basolateral cell boundaries (Fig. 7D,D′).

A distinct characteristic of core PCP proteins is the asymmetric distribution of proteins within polarized cells. Consistent with this, VANGL2 is asymmetrically distributed at the basolateral surface of supporting cells and appears enriched along the side of IPCs facing the cochlear apex when visualized by immunofluorescent labeling using an Airyscan confocal microscopy (Fig. 7I). The asymmetric distribution can be resolved when subsets of IPCs are genetically labeled using *Fgfr3*-iCre^{ER}; *R26R*^{tdTomato} and VANGL2 localization is evaluated at the boundary between labeled and non-labeled IPCs (Fig. 7I) or Deiters cells (Fig. 7J). Because the VANGL2 antibody recognizes a cytosolic epitope, overlap with cytoplasmic tdTomato demonstrates protein localization within labeled cells. As type II fibers pass between the basolateral surfaces of neighboring IPCs, VANGL2 is appropriately positioned to provide polarity information to the migrating growth cone as it initiates the stereotyped turn towards the cochlear base. Consistent with this hypothesis, in *Vangl2* KOs, type II fibers frequently appear bifurcated with projections from the axonal ending directed towards both the cochlear apex and base (Fig. 7K,L).

This type II SGN turning mechanism could be analogous to the PCP signaling event guiding migration of zebrafish FBMNs. Here, VANGL2 distributed along the anterior border of neuroepithelial cells selectively stabilizes FBMN filopodia to promote posterior migration (Davey et al., 2016). If filopodia on one side of type II growth cones are preferentially stabilized because of transient contact with asymmetrically distributed VANGL2, this would bias the growth cone trajectory towards the cochlear base as it passed between neighboring IPCs (Fig. 8A). Alternatively, PCP signaling between IPCs could establish the asymmetric distribution of a classical axon guidance cue (Fig. 8B). In either case, once positioned beneath OHCs, type II SGN peripheral axons are likely to continue extending along this path in response to neurotrophins released by the OHCs. Altogether, these data

Development (2018) 145, dev159012. doi:10.1242/dev.159012

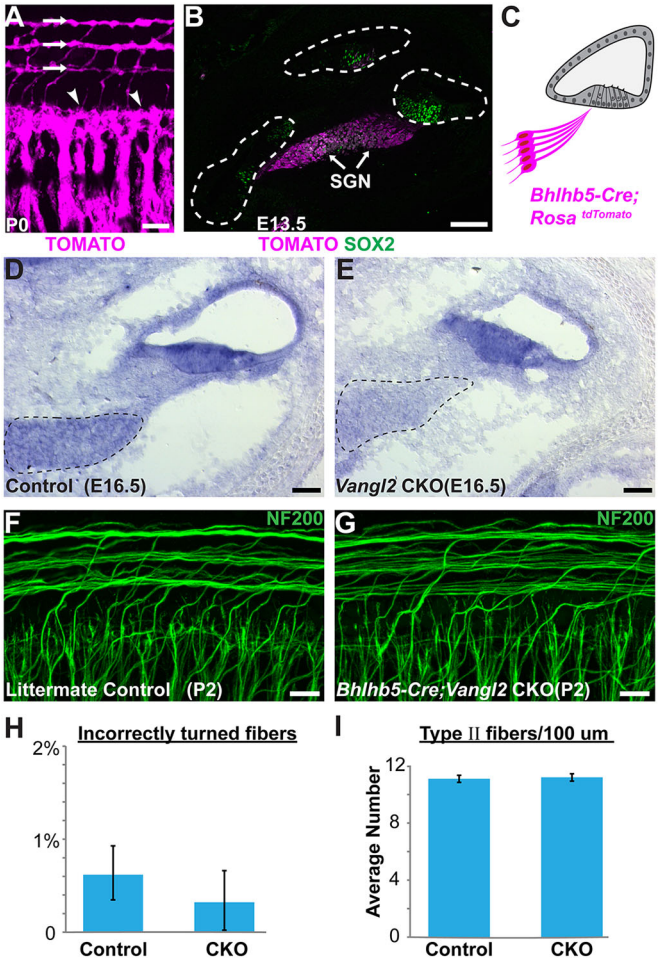

Fig. 5. *Vangl2* is not required in the neuron for peripheral axon turning. (A) Whole-mount immunolabeling of *Bhlhb5*-Cre; *Rosa*^{tdTomato} cochlea at P0 demonstrates reporter activation in both type I (arrowheads) and type II (arrows) peripheral axons. (B) Cross-section of *Bhlhb5*-Cre; *Rosa*^{tdTomato} cochlea at E13.5 demonstrates early recombination in the SGN. At this stage SOX2 immunolabeling delineates the prosensory region of the developing cochlear ducts (dashed outline). (C) Schematic representation of *Bhlhb5*-Cre-mediated recombination in the mouse cochlea. (D,E) *In situ* hybridization demonstrates reduction of *Vangl2* mRNA from *Vangl2* CKO SGNs (dashed outline) but not cochlear duct. (F,G) No type II turning errors were detected in *Bhlhb5*-Cre; *Vangl2* CKOs (n=6) or littermate controls (n=7). (H) No significant differences in the frequency of turning errors between CKOs and littermate controls were detected (P=0.51 by Student's t-test), and (I) the total number of type II fibers innervating the cochlea were unchanged (P=0.73 by Student's t-test). Scale bars: 100 µm in A; 50 µm in D,E; 10 µm in B,F,G.

demonstrate an essential role for PCP signaling in cochlear innervation that is distinct from commissural neuron development in that VANGL2 functions through a non-autonomous mechanism to direct peripheral axon turning.

DISCUSSION

Type II SGN peripheral axons make a characteristic 90° turn towards the cochlear base that is striking in its precision and constancy along the length of the cochlea. In this study, we show that elements of the PCP signaling pathway are required to maintain the fidelity of this axon guidance event. In the absence of *Vangl2*, *Celsr1* and, to a lesser extent, *Fzd3*, the type II fibers frequently turn incorrectly and many project towards the cochlear apex. Owing to the tonotopic organization of cochlea, these incorrectly turned fibers innervate OHCs that detect lower frequency sounds than correctly turned fibers. We further show, using tissue-specific *Vangl2* CKOs, that VANGL2 is required in the supporting cells of the organ of Corti but not in SGNs, and thus acts in a non-autonomous manner. As the type II peripheral axons pass between adjacent IPCs immediately before turning, we propose this subclass of supporting cells to be the site of VANGL2 function. This non-autonomous function distinguishes type II SGNs from commissural axons of the neural tube where VANGL2 and PCP signaling are required in the growth cone (Onishi et al., 2013; Shafer et al., 2011). To account for these phenotypic observations, we propose a model based upon the asymmetric distribution of VANGL2 protein at the basolateral surface of IPCs, in which signaling between IPCs and growth cones biases growth cone trajectories towards the cochlear base (Fig. 8). Although the identity of this signal has not been established, we propose two PCP-dependent candidates. First, transient PCP signaling between VANGL2 in IPCs and FZD3 in growth cones may stabilize filopodia oriented towards the cochlear base before growth cone turning (Fig. 8A). Alternatively, turning is guided by membrane-anchored axon guidance cues asymmetrically distributed through a PCP-dependent mechanism (Fig. 8B). Depending upon its mode of action and location, a conventional axon guidance cue could attract or repel type II SGN growth cones as they passed between the IPCs. In the latter case, the asymmetric distribution of guidance cues would be established by the VANGL2-dependent planar polarization of IPCs. Finally, as the type II peripheral axons pass between the basolateral junctions of supporting cells, they are unlikely to be influenced by structural changes in the apical processes of supporting cells that have been documented upon *Vangl2* gene deletion (Copley et al., 2013).

A significant consequence of this organization is that modular assemblies of core PCP proteins are evenly distributed along the length of the cochlea. Thus, peripheral axons innervating the apical or basal ends of the cochlea receive equivalent guidance cues and do not have to adapt their responsiveness to accommodate extremes of a signaling gradient. The activity of modular assemblies of core PCP proteins has been well described for the apical cell junctions between hair cells and supporting cells, where they coordinate the polarized orientation of stereociliary bundles (Curtin et al., 2003; Montcouquiol et al., 2003; Wang et al., 2006b; Yin et al., 2012). Remarkably, at this location VANGL2 is asymmetrically distributed perpendicular to the neural:abneural axis of the cochlea [Fig. 7B and Montcouquiol et al. (2006)], whereas at the basolateral junctions of supporting cells VANGL2 is parallel to the neural:abneural axis (Fig. 7C), and more similar to PCP protein distribution in non-sensory cells of the greater epithelial ridge (Copley et al., 2013; Goodyear et al., 2017). Finally, as the type II fibers pass beneath the OPCs and Deiters cells, VANGL2 in these supporting cell types is less likely to play a significant role in growth cone turning than VANGL2 in the IPCs. However, the type II peripheral fibers are not restricted to innervating single rows of OHCs and often move between the three outer spiral bundles. In this scenario, the polarized distribution of VANGL2 at junctions between Deiters cells may serve to reinforce the extension of these fibers towards the cochlear base, although determining the specific functions of VANGL2 and PCP signaling in subpopulations of supporting cells awaits the development of additional Cre lines.

During the 90° anterior turning of commissural axons in the spinal cord, PCP proteins, including VANGL2, have been shown to function in the growth cone (Onishi et al., 2013). For commissural axons, the directionality of the turning event depends on an attractive Wnt morphogen gradient established along the anterior

Development (2018) 145, dev159012. doi:10.1242/dev.159012

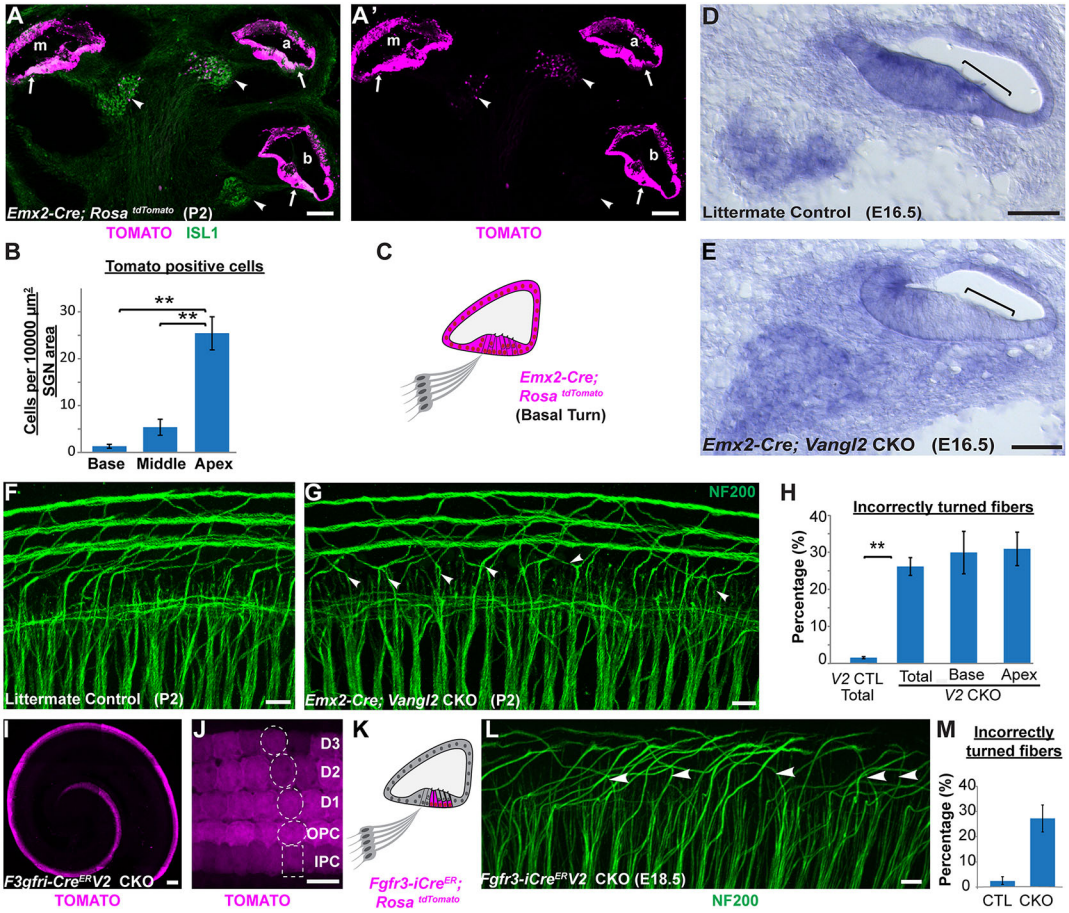

Fig. 6. Vangl2 acts non-autonomously to guide type II SGN peripheral axon turning. (A,A′) Cross-section of an *Emx2*-Cre; *Rosa*^{tdTomato} cochlea at P2 shows Cre-mediated recombination in the apical (a), middle (m) and basal (b) turns of the cochlear duct and organ of Corti (arrows). Limited recombination overlaps with ISL1-immunopositive neurons of the SGN (arrowheads) in a gradient along the length of the cochlea and is more frequent in the apical turn. (B) Quantification of tdTomato activation in the SGN shows a significant decrease from cochlear apex to base. (C) Schematic representation of *Emx2-Cre*-mediated recombination in the cochlear base. (D,E) *In situ* hybridization demonstrates reduction of *Vangl2* mRNA in the *Vangl2* CKO organ of Corti (square brackets) but not in the SGN. (F,G) Turning errors (arrowheads) are frequent in the basal turn of *Emx2*-Cre; *Vangl2* CKOs. (H) Quantification of turning errors throughout the total length of *Vangl2* CKO (*n*=5) cochlea relative to littermate controls (*n*=4), and comparison of turning errors between type II SGNs innervating the base versus apex. (I,J) In *Fgfr3*-iCre^{ER}; Rosa^{tdTomato} cochlea at E18.5, recombination is restricted to supporting cells in the organ of Corti following tamoxifen induction initiated at E14.5. Dashed outlines indicate relative position of each supporting cell type. (K) Schematic representation of *Fgfr3*-iCre^{ER}-mediated recombination in the organ of Corti. (L) Incorrectly turned type II fibers (arrowheads) are readily detected in *Fgfr3-iCre*^{ER}; *Vangl2* CKOs. (M) Quantification of turning errors in the middle turn of the *Fgfr3-iCre*^{ER}; *Vangl2* CKO cochlea (*n*=3) relative to littermate controls (*n*=3). Data are mean±s.e.m. Asterisks show significant differences between genotypes using Student's *t*-test (**P<0.01). Scale bars: 100 µm in A,A′,I; 50 µm in D,E; 10 µm in F,G,J,L.

(high) to posterior (low) axis (Lyuksyutova et al., 2003; Onishi and Zou, 2017). A comparable mechanism in the cochlea would require a cochlear base (high) to apex (low) gradient of Wnt signaling. However, no such gradient has been identified, despite significant interest and effort to find gradients correlated with tonotopy and spiraling along the length of the cochlea (Geng et al., 2016; Sienknecht and Fekete, 2008). Moreover, unlike the case for commissural axons, the type II fibers never fail to turn in PCP mutants and never project beyond the OHCs. These observations suggest that, in the cochlea, a repulsive cue located in its lateral wall may force growth cone turning, and that the role of PCP signaling is to bias turning of the repelled growth cone towards the cochlear base. Once the fibers have turned, they are likely to receive significant neurotrophic support from OHCs (Fritzsch et al., 1997a; Fritzsch et al., 1997b) and would no longer require additional guidance cues. This may explain why incorrectly turned fibers continue to grow robustly, despite projecting in the wrong direction, and are not eliminated by apoptosis (Barclay et al., 2011).

PCP proteins are also linked to the formation of long axon tracks in the mammalian forebrain including the thalamocortical and corticofugal tracks that comprise the internal capsule, the anterior commissure and to a lesser extent the corpus callosum (Qu et al., 2014; Tissir et al., 2005; Wang et al., 2002). In the absence of *Fzd3*, or of *Celsr2* and *Celsr*3, thalamocortical axons and corticofugal axons either fail to cross the diencephalic-telencephalic junction or form whorls at the pallium-subpallium boundary, respectively. CELSR2 and CELSR3 are partially redundant in this system and so, although the loss of *Celsr2* has no effect on its own, the combined loss of *Celsr2* and *Celsr3* enhances the *Celsr3* mutant phenotype such that it resembles that of *Fzd3* mutants (Qu et al., 2014). This is also a non-autonomous event, with FZD3 and CESLR2/3 acting indirectly through a pioneer neuron scaffold that guides subsequent axonal outgrowth (Feng et al., 2016). Although the molecular mechanism underlying subcortical track formation has not been characterized, it does not require *Vangl1* or *Vangl2* (Qu et al., 2014), and is therefore distinct from the *Vangl2*-dependent mechanisms in

Development (2018) 145, dev159012. doi:10.1242/dev.159012

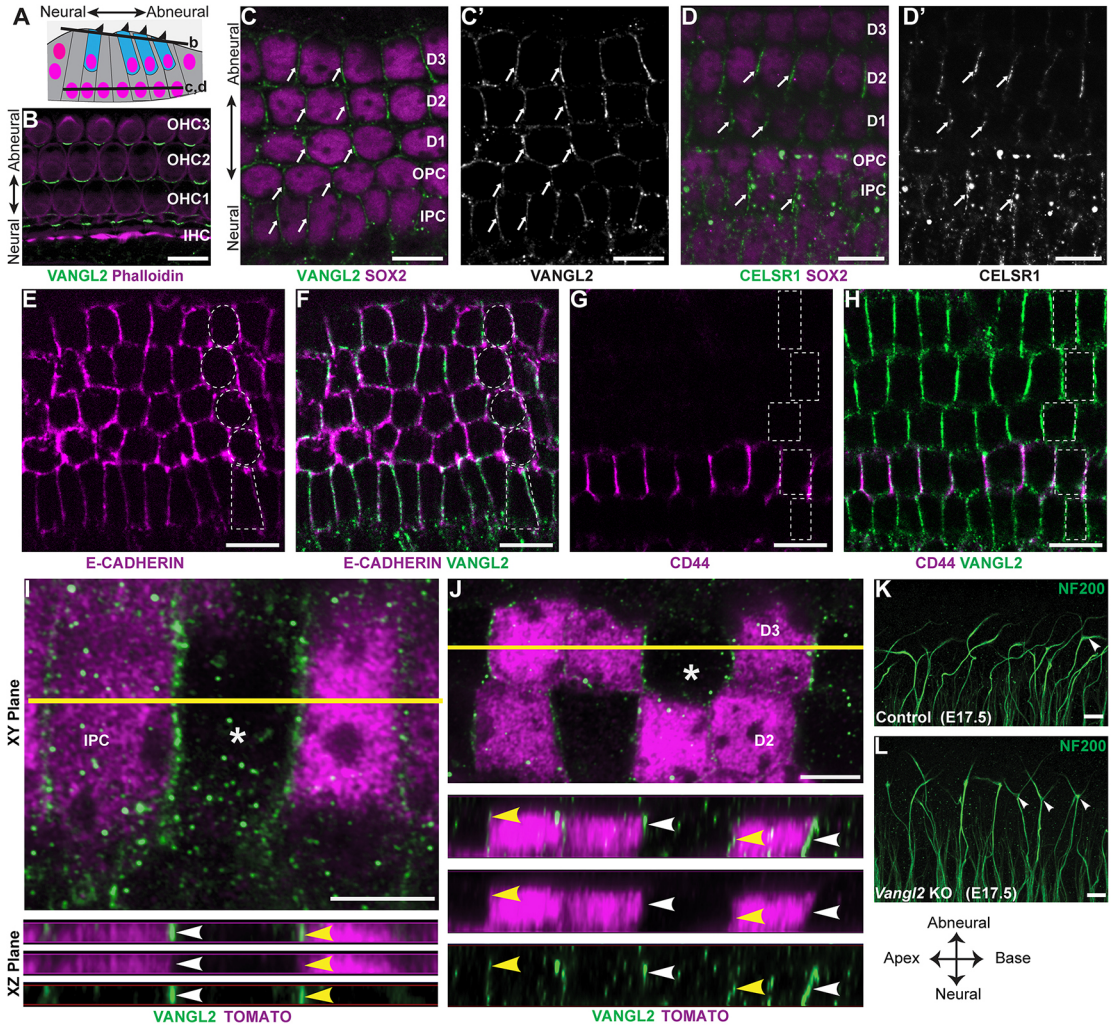

Fig. 7. Vangl2 is asymmetrically distributed along the basolateral wall of supporting cells. (A) Schematic representation of the organ of Corti highlighting the relative position of hair cells (blue) and supporting cells (gray), and the 'z-position' of optical sections corresponding to B-D. (B) At the apical surface of the organ of Corti, VANGL2 is asymmetrically distributed at hair cell to supporting cell boundaries, perpendicular to the neural:abneural axis of the cochlea. The organization of hair cells and supporting cells is revealed by phalloidin staining of filamentous actin. (C,C′) At deeper *z*-positions, VANGL2 is asymmetrically distributed at cell boundaries (arrows) between the basolateral walls of supporting cells, identified by SOX2 immunolabeling. At this *z*-position, VANGL2 is asymmetrically distributed at boundaries oriented parallel to the neural:abneural axis of the cochlea. (D,D′) The distribution of CELSR1 (arrows) is similar to VANGL2 at boundaries between neighboring supporting cells. (E,F) Colocalization with the basolateral marker E-cadherin (magenta) confirms the basolateral distribution of VANGL2 (green). (G,H) Immunolabeling for the OPC-specific marker CD44 (magenta) confirms that, in this *z*-position, VANGL2 (green) is present at intercellular junctions between neighboring supporting cells. (I) Super-resolution imaging of VANGL2 at the boundaries between IPCs following sparse genetic labeling by *Fgfr3*-iCre^{ER}; *tdTomato* to resolve the border between neighboring cells. Asterisk shows a wild-type cell flanked by labeled cells. Yellow line marks the position of projections further evaluated in the *xz* plane. Arrowheads indicate the asymmetric distribution of VANGL2 on one side of wild-type (white) or *Fgfr3*-iCre^{ER}-labeled (yellow) IPCs facing the cochlear apex. (J) Super-resolution imaging of VANGL2 at the boundaries between Dieters cells (D3) following sparse genetic labeling by *Fgfr3*-iCre^{ER}; *tdTomato*. Asterisk shows a wild-type cell flanked by labeled cells. Yellow line marks the position of projections further evaluated in the *xz* plane. Arrowheads indicate the asymmetric distribution of VANGL2 on the side of wild-type (white) or *Fgfr3*-iCre^{ER}-labeled (yellow) IPCs facing the cochlear apex. (K,L) Frequent appearance of bifurcated growth cones (arrowheads) in the middle turn of cochlea from E17.5 *Vangl2* KOs compared with the littermate controls. Dashed outlines indicate the relative position of supporting cells. Scale bars: 10 µm in B-H,K,L; 5 µm in I,J. The anatomical reference applies to B-L.

the cochlea and neural tube. Thus, the contribution of Vangl2 to type II fiber turning is mechanistically different from two previously described PCP-dependent innervation events: commissural axon pathfinding and subcortical axon track formation.

Type II fiber turning in the cochlea is also unique because it is impacted by the loss of *Celsr1*. In contrast to *Celsr2* and *Celsr3*, *Celsr1* is thought to exclusively regulate epithelial PCP, and mutant phenotypes relating to axon guidance have not been reported outside of what we describe for the cochlea (Goffinet and Tissir, 2017). In its capacity as a PCP signaling factor, CELSR1 is thought to bridge neighboring cells and thereby facilitate PCP signaling between them. One possibility is that CELSR1 facilitates a transient PCP signaling complex comprising VANGL2 in IPCs and FZD3 in the growth cone passing through this region (Fig. 8A). Alternatively, CELSR1 guides growth cone turning indirectly by establishing PCP signaling along the length of the cochlea in the epithelial-like supporting cells. In this latter case, we predict that a classic axon guidance cue might be directing type II fiber turning, and that the polarized distribution of this cue is PCP dependent (Fig. 8B).

PCP signaling is also required for the caudal migration of FBMNs from their site of mitosis in rhombomere 4 to the future site of the

Development (2018) 145, dev159012. doi:10.1242/dev.159012

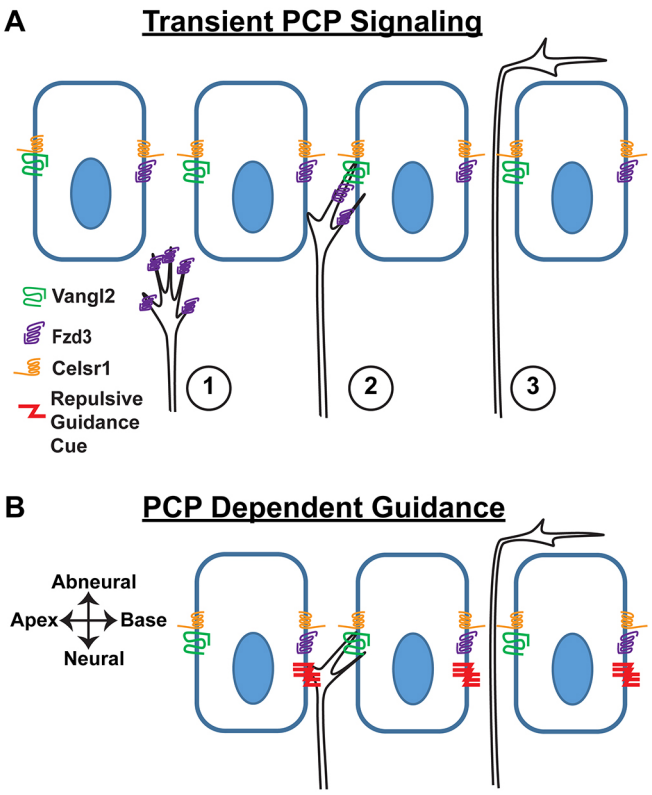

Fig. 8. Alternative models for the non-autonomous function of VANGL2 in cochlear innervation. (A) Transient PCP signaling between FZD3 in the type II SGN growth cone and asymmetrically distributed VANGL2 at the basolateral surface of IPCs influences growth cone dynamics such that extension of the peripheral axon is biased towards the cochlear base. In this model, the asymmetric enrichment of VANGL2 on the side of IPCs facing the cochlear apex stabilizes filopodial extensions on the side of the growth cone facing the cochlear base, thereby promoting axon turning in this direction. Numbering represents the sequential progression of transient PCP signaling. (B) Alternatively, classical axon guidance molecules (represented here by a repulsive cue) may be asymmetrically distributed at supporting cell boundaries through a PCP-dependent mechanism. Depending upon the mode of action and location, these molecules could direct growth cone turning towards the cochlear base.

facial motor nucleus in rhombomere 6. In the absence of *Vangl2* in mouse (Glasco et al., 2012) and zebrafish (Jessen et al., 2002), many FBMNs migrate incorrectly to more rostral locations. In zebrafish, PCP proteins are proposed to have dual cell-autonomous and non-cell-autonomous functions during this process (Davey et al., 2016). The non-autonomous function resembles type II peripheral axon turning, because asymmetrically distributed VANGL2 in the environment directs the initial movement of FBMNs by stabilizing filopodia at the leading edge of the cell (Davey et al., 2016). This involves asymmetric intercellular interactions between FZD3 and VANGL2, such that filopodia containing FZD3 that contact VANGL2 in the environment are selectively stabilized. Because of the similar dynamic nature of filopodia in migrating cells and neuronal growth cones, it is tempting to speculate that the turning of type II fibers similarly occurs through stabilization of filopodia by VANGL2, in this case those filopodia extending from the side of the growth cone facing the cochlear base. In addition, both type II SGNs and FBMNs require CELSR1 and are not impacted by the loss of *Celsr3* (Qu et al., 2010). However, in contrast to FBMN migration, where VANGL2 also has an autonomous function (Davey et al., 2016; Walsh et al., 2011), we provide genetic evidence that type II SGNs do not require VANGL2 in the growth cone for turning to occur. Thus, it is possible that type II fiber turning is directed by a cochlear-centric mechanism of PCP signaling that is distinct from that proposed for forebrain wiring, commissural axon pathfinding or FBMN migration. Whether this is an indirect outcome of the planar polarization of inner ear epithelia or a transient PCP signal conveyed between supporting cells and the growth cone will require additional research.

The type II neurons constitute a small proportion of the spiral ganglion that have been assigned important nociceptive or neuroprotective functions. Although the physiological significance of the basal turn of the type II peripheral axon is not understood, turning allows the neuron to pool input from 10-15 OHCs, and detect sound across a quarter octave of higher frequencies than type I fibers with comparable radial projections. More significantly, deafness resulting from acoustic trauma is associated with pathologies in the SGN (Liberman, 1990), and the retraction of peripheral axons and loss of synapses following exposure to moderately loud noise can also lead to hearing loss (Kujawa and Liberman, 2015). Restoring hearing involves coaxing SGNs to re-innervate their hair cell partners in order to restore sensory input to the CNS, and rebuilding the neuroprotective type II circuitry is an important aspect of this effort. It is broadly accepted that hair cell re-innervation will employ similar molecular mechanisms, including PCP signaling, that occur during embryonic development. Therefore, completely understanding these developmental processes is an important and essential prerequisite for regeneration-based therapeutic strategies.

MATERIALS AND METHODS

Mouse strains and husbandry

Vangl2 KO (Yin et al., 2012) and *Fzd3* KO (Wang et al., 2002) embryos were generated by intercrossing heterozygous breeding pairs. *Vangl2* CKOs for mutant phenotyping were generated by intercrossing *Vangl2*^{floxed} female mice with *Vangl2*$^{\Delta TMs/wt}$ male mice expressing tissue-specific Cre recombinase as previously described (Copley et al., 2013). For these studies, *Pax2*-Cre mice (Ohyama and Groves, 2004) were provided by A. Groves (Baylor College of Medicine, Houston, TX, USA), *Bhlhb5*-Cre mice (Ross et al., 2010) were provided by M. Greenberg (Harvard Medical School, Boston, MA, USA), and *Emx2*^{Cre} mice (Kimura et al., 2005) were provided by S. Aizawa (Riken Institute, Wako, Japan). *Vangl2* CKOs for validation of Cre-mediated gene deletion were generated by intercrossing *Vangl2*^{floxed} female mice with *Vangl2*$^{LoxP/wt}$ male mice expressing *Emx2*-Cre or *Bhlhb5*-Cre. *Pax2*-Cre; *Vangl1*; *Vangl2* CKOs were generated by crossing *Pax2*-Cre; *Vangl1*$^{\Delta TMs/wt}$; *Vangl2*$^{\Delta TMs/wt}$ males with *Vangl1*^{floxed}; *Vangl2*^{floxed} females. The *Vangl1* floxed line (Wang et al., 2016) was provided by J. Nathans (Johns Hopkins University, Baltimore, MD, USA), and the *Vangl1*$^{\Delta TMs}$ allele derived using constitutive CMV-Cre (Schwenk et al., 1995). *Celsr1* KO (Ravni et al., 2009), *Celsr3* KO (Tissir et al., 2005) and littermate control tissue were provided by F. Tissir (Université Catholique de Louvain, Brussels, Belgium). *Fgfr3-iCre*^{ER} (Young et al., 2010) was crossed with *R26R-tdTomato* reporter mice (Madisen et al., 2010) to generate *Fgfr3-iCre*$^{ER+}$; *R26R*$^{tdTomato/WT}$ tissue for the study of VANGL2 protein localization. *Fgfr3-iCre*^{ER} was activated with a single intraperitoneal injection of 1 mg tamoxifen at E16.5. Three daily doses of 2 mg from E14.5 to E16.5 were administered for *Vangl2* CKO induction. For timed breeding and tissue staging, noon on the day in which vaginal plug is seen was considered E0.5 and the day mice were born was considered P0. Mice from either sex were used for experimentation. Mice were maintained at the University of Utah under IACUC approved guidelines, and genotyped using allele-specific PCR reactions.

Immunofluorescence

Inner ear tissues were fixed using 4% paraformaldehyde prepared in 67 mM Sorenson's phosphate buffer (pH 7.4) for 2 h on ice. For whole-mount immunofluorescent labeling, the cochlea was micro-dissected and detergent-permeabilized using blocking solution (5% normal donkey

Development (2018) 145, dev159012. doi:10.1242/dev.159012

serum, 1% BSA, in PBS) supplemented with 0.5% Triton-X100. Primary antibodies and phalloidin Alexa Fluor 488 (Invitrogen, A12379, 1:1000) were diluted in blocking solution supplemented with 0.1% Tween-20 and incubated overnight at 4°C. Tissue was washed thoroughly using PBS with 0.05% Tween-20 and incubated with species-specific Alexa-conjugated secondary antibodies (Invitrogen, A21206, A21202, A21208, A10042, A11057, A31573, A31571, all diluted 1:1500), washed and mounted for fluorescence microscopy using Prolong Gold (Molecular Probes). For cryosections, tissue was cryoprotected by passing through a post-fixation sucrose gradient, frozen in Neg50 (Richard Allan Scientific) and sectioned at 20 µm using a Leica CM3050 cryostat. Immunolabeling on slides was completed using the same labeling protocol in the absence of Tween-20. Fluorescent images were acquired using structured illumination microscopy with a Zeiss Axio Imager M.2 with ApoTome.2 attachment and an Axiocam 506 mono camera, and images were processed using Zeiss Zen software followed by figure preparation with Adobe Illustrator. Super-resolution imaging using a Zeiss LSM 880 Airyscan was performed at the Fluorescence Microscopy Core Facility, part of the Health Sciences Cores at the University of Utah.

Commercial antibodies used in this study were: rat anti-E-cadherin (Invitrogen, 13-1900, 1:1000), rat anti-CD44 (BD Biosciences, 550538, 1:750), mouse anti-islet 1 (DSHB, 39.3F7, deposited by T. M. Jessell and S. Brenner-Morton, 1:100), mouse anti-myosin 7a (DSHB, 138-1 deposited by D. J. Orten, 1:100), rabbit anti-NF200 (Millipore, AB1989, 1:1500), rat anti-tdTOMATO (Kerafast, EST203, 1:2000) and goat anti-SOX2 (Santa-Cruz, sc17320, 1:100). Guinea pig anti-CELSR1 [Devenport and Fuchs (2008), 1:250] was a gift from D. Devenport (Princeton University, NJ, USA) and rabbit anti-VANGL2 [Montcouquiol et al. (2006), 1:1500] was a gift from M. Montcouquiol (Université Bordeaux, France).

DiI tracing

Cochlear tissues were fixed and microdissected as described for immunofluorescent labeling without detergents, maintaining connections between the SGN and organ of Corti. To label small groups of neurons, microdissection pins were dipped into 1 mg/m DiI (ThermoFisher, D3911) solution prepared in DMSO and inserted in the SGN region of the microdissected cochlea. Tissue was then maintained in 1×PBS and incubated at room temperature for 20-24 h before mounting for fluorescence microscopy using 30% sucrose.

Quantification of peripheral axon turning defects

Type II peripheral axons were identified for quantification based upon morphological criteria following NF200 labeling. Growth cone turning was evaluated in the region between the termination of type I fibers at the IHCs and the first outer spiral bundle beneath OHC1. For postnatal samples, fibers were evaluated in the basal, middle and apical turn in regions corresponding to 25%, 50% and 75% of the cochlear length running from base to apex. Individual fibers were analyzed from all three regions (on average 33 peripheral axons were analyzed per region) and pooled (on average 99 axons per cochlea) to generate a single error frequency measure that was subsequently averaged between biological replicates from each genotype. In some instances, as indicated in the figure legends, cochlear regions were analyzed independently (on average 37 peripheral axons were analyzed per region) to assay for differences along the length of the cochlea. For E18.5 samples, evaluation was restricted to the basal turn of the cochlea, as type II peripheral axon turning occurs in a developmental gradient from base to apex, and fibers in more apical locations had not yet turned at this stage. A minimum of three animals were used for each genotype and six *Bhlhb5*-Cre; *Vangl2* CKOs were analyzed to validate this negative result. Between all genotypes and ages evaluated, a total number of 112 cochleas were assayed. Student's *t*-test (unpaired with equal variance) and one-way ANOVA analyses were used to determine the statistical significance of differences between KOs and littermate controls, and between different cochlear regions of KOs, respectively.

In situ hybridization

Embryonic heads were fixed using 4% paraformaldehyde prepared in 1× PBS (pH 7.4) overnight at 4°C, cryoprotected by passing through a post-fixation sucrose gradient, frozen in Neg50 (Richard Allan Scientific) and sectioned at 20 µm using a Leica CM3050 cryostat. Sections were blocked, permeabilized and hybridized with digoxgenin-labeled anti-sense probes, which were detected using alkaline phosphatase-conjugated anti-digoxigenin antibodies (Roche). Following alkaline phosphatase detection, sections were imaged using the Zeiss Axio Imager M.2 and Axiocam 105 color camera. See supplementary Materials and Methods for detailed *in situ* hybridization protocols. To evaluate *Vangl2* mRNA distribution in wild-type mice, a *Vangl2* probe template was generated by PCR amplification of whole embryo cDNA using the following primer pair: 5′-CGGGGCCTCGAGGGGGAAAC-3′; 5′-CCCGGAGCCTGGATCGT-CACTGA-3′. These were TOPO-cloned into a plasmid containing a T7 and SP6 promoter. To evaluate *Vangl2* mRNA distribution in *Vangl2* CKOs, a smaller Vangl2 probe restricted to coding sequence exons 2 and 3, which are flanked by LoxP sites and eliminated in *Vangl2* CKO lines, was derived from the larger wild-type probe template. *Fzd3*, *Celrs1*, *Celsr2* and *Celsr3* probe templates were provided by F. Tissir (Tissir et al., 2002; Tissir and Goffinet, 2006).

Acknowledgements

We thank Fadel Tissir for providing *Celsr1* and *Celsr3* mutant tissue and ISH probe templates, and Orvelin Roman, Jr for animal care and genotyping.

Competing interests

The authors declare no competing or financial interests.

Author contributions

Conceptualization: S.R.G., M.R.D.; Methodology: S.R.G., E.M.R.; Validation: S.R.G., E.M.R., M.R.D.; Formal analysis: S.R.G.; Investigation: S.R.G., E.M.R.; Writing - original draft: S.R.G.; Writing - review & editing: M.R.D.; Visualization: S.R.G., E.M.R., M.R.D.; Supervision: M.R.D.; Project administration: M.R.D.; Funding acquisition: M.R.D.

Funding

This work was supported by the National Institutes of Health (R01DC013066 and R21DC015635 to M.R.D., and T32HD007491 to E.M.R.). Microscopy equipment was obtained using the National Center for Research Resources Shared Equipment Grant (1S10RR024761-01). Deposited in PMC for release after 12 months.

Supplementary information

Supplementary information available online at
http://dev.biologists.org/lookup/doi/10.1242/dev.159012.supplemental

References

Anttonen, T., Kirjavainen, A., Belevich, I., Laos, M., Richardson, W. D., Jokitalo, E., Brakebusch, C. and Pirvola, U. (2012). Cdc42-dependent structural development of auditory supporting cells is required for wound healing at adulthood. *Sci. Rep.* **2**, 978.

Appler, J. M. and Goodrich, L. V. (2011). Connecting the ear to the brain: molecular mechanisms of auditory circuit assembly. *Prog. Neurobiol.* **93**, 488-508.

Appler, J. M., Lu, C. C., Druckenbrod, N. R., Yu, W.-M., Koundakjian, E. J. and Goodrich, L. V. (2013). Gata3 is a critical regulator of cochlear wiring. *J. Neurosci.* **33**, 3679-3691.

Barclay, M., Ryan, A. F. and Housley, G. D. (2011). Type I vs type II spiral ganglion neurons exhibit differential survival and neuritogenesis during cochlear development. *Neural Dev.* **6**, 33.

Bashaw, G. J. and Klein, R. (2010). Signaling from axon guidance receptors. *Cold Spring Harbor Perspect. Biol.* **2**, a001941.

Berglund, A. and Ryugo, D. K. (1987). Hair cell innervation by spiral ganglion neurons in the mouse. *J. Comp. Neurol.* **255**, 560-570.

Bovolenta, P. and Dodd, J. (1990). Guidance of commissural growth cones at the floor plate in embryonic rat spinal cord. *Development* **109**, 435-447.

Coate, T. M., Spita, N. A., Zhang, K. D., Isgrig, K. T. and Kelley, M. W. (2015). Neuropilin-2/Semaphorin-3F-mediated repulsion promotes inner hair cell innervation by spiral ganglion neurons. *eLife* **4**, e07830.

Copley, C. O., Duncan, J. S., Liu, C., Cheng, H. and Deans, M. R. (2013). Postnatal refinement of auditory hair cell planar polarity deficits occurs in the absence of Vangl2. *J. Neurosci.* **33**, 14001-14016.

Curtin, J. A., Quint, E., Tsipouri, V., Arkell, R. M., Cattanach, B., Copp, A. J., Henderson, D. J., Spurr, N., Stanier, P., Fisher, E. M. et al. (2003). Mutation of Celsr1 disrupts planar polarity of inner ear hair cells and causes severe neural tube defects in the mouse. *Curr. Biol.* **13**, 1129-1133.

Davey, C. F. and Moens, C. B. (2017). Planar cell polarity in moving cells: think globally, act locally. *Development* **144**, 187-200.
Davey, C. F., Mathewson, A. W. and Moens, C. B. (2016). PCP signaling between migrating neurons and their planar-polarized neuroepithelial environment controls filopodial dynamics and directional migration. *PLoS Genet.* **12**, e1005934.
Defourny, J., Poirrier, A.-L., Lallemend, F., Sánchez, S. M., Neef, J., Vanderhaeghen, P., Soriano, E., Peuckert, C., Kullander, K. and Fritzsch, B. (2013). Ephrin-A5/EphA4 signalling controls specific afferent targeting to cochlear hair cells. *Nat. Commun.* **4**, 1438.
Devenport, D. and Fuchs, E. (2008). Planar polarization in embryonic epidermis orchestrates global asymmetric morphogenesis of hair follicles. *Nat. Cell Biol.* **10**, 1257-1268.
Druckenbrod, N. R. and Goodrich, L. V. (2015). Sequential retraction segregates SGN processes during target selection in the cochlea. *J. Neurosci.* **35**, 16221-16235.
Duncan, J. S., Stoller, M. L., Francl, A. F., Tissir, F., Devenport, D. and Deans, M. R. (2017). Celsr1 coordinates the planar polarity of vestibular hair cells during inner ear development. *Dev. Biol.* **423**, 126-137.
Feng, J., Xian, Q., Guan, T., Hu, J., Wang, M., Huang, Y., So, K. F., Evans, S. M., Chai, G., Goffinet, A. M. et al. (2016). Celsr3 and Fzd3 organize a pioneer neuron scaffold to steer growing thalamocortical axons. *Cereb. Cortex* **26**, 3323-3334.
Fenstermaker, A. G., Prasad, A. A., Bechara, A., Adolfs, Y., Tissir, F., Goffinet, A., Zou, Y. and Pasterkamp, R. J. (2010). Wnt/planar cell polarity signaling controls the anterior-posterior organization of monoaminergic axons in the brainstem. *J. Neurosci.* **30**, 16053-16064.
Flores, E. N., Duggan, A., Madathany, T., Hogan, A. K., Márquez, F. G., Kumar, G., Seal, R. P., Edwards, R. H., Liberman, M. C. and García-Añoveros, J. (2015). A non-canonical pathway from cochlea to brain signals tissue-damaging noise. *Curr. Biol.* **25**, 606-612.
Fritzsch, B., Fariñas, I. and Reichardt, L. F. (1997a). Lack of neurotrophin 3 causes losses of both classes of spiral ganglion neurons in the cochlea in a region-specific fashion. *J. Neurosci.* **17**, 6213-6225.
Fritzsch, B., Silos-Santiago, I., Bianchi, L. and Farinas, I. (1997b). The role of neurotrophic factors in regulating the development of inner ear innervation. *Trends Neurosci.* **20**, 159-164.
Froud, K. E., Wong, A. C. Y., Cederholm, J. M. E., Klugmann, M., Sandow, S. L., Julien, J.-P., Ryan, A. F. and Housley, G. D. (2015). Type II spiral ganglion afferent neurons drive medial olivocochlear reflex suppression of the cochlear amplifier. *Nat. Commun.* **6**.
Geng, R., Noda, T., Mulvaney, J. F., Lin, V. Y., Edge, A. S. and Dabdoub, A. (2016). Comprehensive expression of Wnt signaling pathway genes during development and maturation of the mouse cochlea. *PLoS ONE* **11**, e0148339.
Glasco, D. M., Sittaramane, V., Bryant, W., Fritzsch, B., Sawant, A., Paudyal, A., Stewart, M., Andre, P., Cadete Vilhais-Neto, G., Yang, Y. et al. (2012). The mouse Wnt/PCP protein Vangl2 is necessary for migration of facial branchiomotor neurons, and functions independently of Dishevelled. *Dev. Biol.* **369**, 211-222.
Goffinet, A. M. and Tissir, F. (2017). Seven pass Cadherins CELSR1-3. *Semin. Cell Dev. Biol.* **69**, 102-110.
Goodyear, R. J., Lu, X., Deans, M. R. and Richardson, G. P. (2017). A tectorin-based matrix and planar cell polarity genes are required for normal collagen-fibril orientation in the developing tectorial membrane. *Development* **144**, 3978-3989.
Hertzano, R., Puligilla, C., Chan, S.-L., Timothy, C., Depireux, D. A., Ahmed, Z., Wolf, J., Eisenman, D. J., Friedman, T. B., Riazuddin, S. et al. (2010). CD44 is a marker for the outer pillar cells in the early postnatal mouse inner ear. *J. Assoc. Res. Otolaryngol.* **11**, 407-418.
Huang, L. C., Thorne, P. R., Housley, G. D. and Montgomery, J. M. (2007). Spatiotemporal definition of neurite outgrowth, refinement and retraction in the developing mouse cochlea. *Development* **134**, 2925-2933.
Jessen, J. R., Topczewski, J., Bingham, S., Sepich, D. S., Marlow, F., Chandrasekhar, A. and Solnica-Krezel, L. (2002). Zebrafish trilobite identifies new roles for Strabismus in gastrulation and neuronal movements. *Nat. Cell Biol.* **4**, 610-615.
Kim, Y. J., Wang, S.-Z., Tymanskyj, S., Ma, L., Tao, H. W. and Zhang, L. I. (2016). Dcc mediates functional assembly of peripheral auditory circuits. *Sci. Rep.* **6**, 23799.
Kimura, J., Suda, Y., Kurokawa, D., Hossain, Z. M., Nakamura, M., Takahashi, M., Hara, A. and Aizawa, S. (2005). Emx2 and Pax6 function in cooperation with Otx2 and Otx1 to develop caudal forebrain primordium that includes future archipallium. *J. Neurosci.* **25**, 5097-5108.
Koundakjian, E. J., Appler, J. L. and Goodrich, L. V. (2007). Auditory neurons make stereotyped wiring decisions before maturation of their targets. *J. Neurosci.* **27**, 14078-14088.
Kujawa, S. G. and Liberman, M. C. (2015). Synaptopathy in the noise-exposed and aging cochlea: Primary neural degeneration in acquired sensorineural hearing loss. *Hear. Res.* **330**, 191-199.
Liberman, M. C. (1990). Quantitative assessment of inner ear pathology following ototoxic drugs or acoustic trauma. *Toxicol. Pathol.* **18**, 138-148.
Liu, C., Glowatzki, E. and Fuchs, P. A. (2015). Unmyelinated type II afferent neurons report cochlear damage. *Proc. Natl Acad. Sci. USA* **112**, 14723-14727.
Lyuksyutova, A. I., Lu, C. C., Milanesio, N., King, L. A., Guo, N., Wang, Y., Nathans, J., Tessier-Lavigne, M. and Zou, Y. (2003). Anterior-posterior guidance of commissural axons by Wnt-frizzled signaling. *Science* **302**, 1984-1988.
Madisen, L., Zwingman, T. A., Sunkin, S. M., Oh, S. W., Zariwala, H. A., Gu, H., Ng, L. L., Palmiter, R. D., Hawrylycz, M. J., Jones, A. R. et al. (2010). A robust and high-throughput Cre reporting and characterization system for the whole mouse brain. *Nat. Neurosci.* **13**, 133-140.
Maison, S., Liberman, L. D. and Liberman, M. C. (2016). Type II cochlear ganglion neurons do not drive the olivocochlear reflex: re-examination of the cochlear phenotype in peripherin knock-out mice. *eNeuro* **3**, ENEURO 0207-16.2016.
Montcouquiol, M., Rachel, R. A., Lanford, P. J., Copeland, N. G., Jenkins, N. A. and Kelley, M. W. (2003). Identification of Vangl2 and Scrb1 as planar polarity genes in mammals. *Nature* **423**, 173-177.
Montcouquiol, M., Sans, N., Huss, D., Kach, J., Dickman, J. D., Forge, A., Rachel, R. A., Copeland, N. G., Jenkins, N. A., Bogani, D. et al. (2006). Asymmetric localization of Vangl2 and Fz3 indicate novel mechanisms for planar cell polarity in mammals. *J. Neurosci.* **26**, 5265-5275.
Nayagam, B. A., Muniak, M. A. and Ryugo, D. K. (2011). The spiral ganglion: connecting the peripheral and central auditory systems. *Hear. Res.* **278**, 2-20.
O'donnell, M., Chance, R. K. and Bashaw, G. J. (2009). Axon growth and guidance: receptor regulation and signal transduction. *Annu. Rev. Neurosci.* **32**, 383-412.
Ohyama, T. and Groves, A. K. (2004). Generation of Pax2-Cre mice by modification of a Pax2 bacterial artificial chromosome. *Genesis* **38**, 195-199.
Onishi, K. and Zou, Y. (2017). Sonic Hedgehog switches on Wnt/planar cell polarity signaling in commissural axon growth cones by reducing levels of Shisa2. *eLife* **6**, e25269.
Onishi, K., Shafer, B., Lo, C., Tissir, F., Goffinet, A. M. and Zou, Y. (2013). Antagonistic functions of Dishevelleds regulate Frizzled3 endocytosis via filopodia tips in Wnt-mediated growth cone guidance. *J. Neurosci.* **33**, 19071-19085.
Ono, K., Kita, T., Sato, S., O'Neill, P., Mak, S.-S., Paschaki, M., Ito, M., Gotoh, N., Kawakami, K. and Sasai, Y. (2014). FGFR1-Frs2/3 signalling maintains sensory progenitors during inner ear hair cell formation. *PLoS Genet.* **10**, e1004118.
Qu, Y., Glasco, D. M., Zhou, L., Sawant, A., Ravni, A., Fritzsch, B., Damrau, C., Murdoch, J. N., Evans, S., Pfaff, S. L. et al. (2010). Atypical cadherins Celsr1-3 differentially regulate migration of facial branchiomotor neurons in mice. *J. Neurosci.* **30**, 9392-9401.
Qu, Y., Huang, Y., Feng, J., Alvarez-Bolado, G., Grove, E. A., Yang, Y., Tissir, F., Zhou, L. and Goffinet, A. M. (2014). Genetic evidence that Celsr3 and Celsr2, together with Fzd3, regulate forebrain wiring in a Vangl-independent manner. *Proc. Natl. Acad. Sci. USA* **111**, E2996-E3004.
Raphael, Y. and Altschuler, R. A. (2003). Structure and innervation of the cochlea. *Brain Res. Bull.* **60**, 397-422.
Ravni, A., Qu, Y., Goffinet, A. M. and Tissir, F. (2009). Planar cell polarity cadherin Celsr1 regulates skin hair patterning in the mouse. *J. Invest. Dermatol.* **129**, 2507.
Riccomagno, M. M. and Kolodkin, A. L. (2015). Sculpting neural circuits by axon and dendrite pruning. *Annu. Rev. Cell Dev. Biol.* **31**, 779-805.
Ross, S. E., Mardinly, A. R., Mccord, A. E., Zurawski, J., Cohen, S., Jung, C., Hu, L., Mok, S. I., Shah, A. and Savner, E. M. (2010). Loss of inhibitory interneurons in the dorsal spinal cord and elevated itch in Bhlhb5 mutant mice. *Neuron* **65**, 886-898.
Schwenk, F., Baron, U. and Rajewsky, K. (1995). A cre-transgenic mouse strain for the ubiquitous deletion of loxP-flanked gene segments including deletion in germ cells. *Nucleic Acids Res.* **23**, 5080-5081.
Shafer, B., Onishi, K., Lo, C., Colakoglu, G. and Zou, Y. (2011). Vangl2 promotes Wnt/planar cell polarity-like signaling by antagonizing Dvl1-mediated feedback inhibition in growth cone guidance. *Dev. Cell* **20**, 177-191.
Shima, Y., Copeland, N. G., Gilbert, D. J., Jenkins, N. A., Chisaka, O., Takeichi, M. and Uemura, T. (2002). Differential expression of the seven-pass transmembrane cadherin genes Celsr1-3 and distribution of the Celsr2 protein during mouse development. *Dev. Dyn.* **223**, 321-332.
Sienknecht, U. J. and Fekete, D. M. (2008). Comprehensive Wnt-related gene expression during cochlear duct development in chicken. *J. Comp. Neurol.* **510**, 378-395.
Sittaramane, V., Pan, X., Glasco, D. M., Huang, P., Gurung, S., Bock, A., Li, S., Wang, H., Kawakami, K., Matise, M. P. et al. (2013). The PCP protein Vangl2 regulates migration of hindbrain motor neurons by acting in floor plate cells, and independently of cilia function. *Dev. Biol.* **382**, 400-412.
Song, H., Hu, J., Chen, W., Elliott, G., Andre, P., Gao, B. and Yang, Y. (2010). Planar cell polarity breaks bilateral symmetry by controlling ciliary positioning. *Nature* **466**, 378-382.
Stoller, M. L., Roman, O., Jr. and Deans, M. R. (2018). Domineering non-autonomy in Vangl1;Vangl2 double mutants demonstrates intercellular PCP signaling in the vertebrate inner ear. *Dev. Biol.* **437**, 17-26.
Tissir, F. and Goffinet, A. M. (2006). Expression of planar cell polarity genes during development of the mouse CNS. *Eur. J. Neurosci.* **23**, 597-607.

Tissir, F., De-Backer, O., Goffinet, A. M. and Lambert De Rouvroit, C. (2002). Developmental expression profiles of Celsr (Flamingo) genes in the mouse. *Mech. Dev.* **112**, 157-160.
Tissir, F., Bar, I., Jossin, Y., De Backer, O. and Goffinet, A. M. (2005). Protocadherin Celsr3 is crucial in axonal tract development. *Nat. Neurosci.* **8**, 451-457.
Torban, E., Patenaude, A.-M., Leclerc, S., Rakowiecki, S., Gauthier, S., Andelfinger, G., Epstein, D. J. and Gros, P. (2008). Genetic interaction between members of the Vangl family causes neural tube defects in mice. *Proc. Natl. Acad. Sci. USA* **105**, 3449-3454.
Wada, H., Tanaka, H., Nakayama, S., Iwasaki, M. and Okamoto, H. (2006). Frizzled3a and Celsr2 function in the neuroepithelium to regulate migration of facial motor neurons in the developing zebrafish hindbrain. *Development* **133**, 4749-4759.
Walsh, G. S., Grant, P. K., Morgan, J. A. and Moens, C. B. (2011). Planar polarity pathway and Nance-Horan syndrome-like 1b have essential cell-autonomous functions in neuronal migration. *Development* **138**, 3033-3042.
Wang, Y. S., Thekdi, N., Smallwood, P. M., Macke, J. P. and Nathans, J. (2002). Frizzled-3 is required for the development of major fiber tracts in the rostral CNS. *J. Neurosci.* **22**, 8563-8573.
Wang, J., Hamblet, N. S., Mark, S., Dickinson, M. E., Brinkman, B. C., Segil, N., Fraser, S. E., Chen, P., Wallingford, J. B. and Wynshaw-Boris, A. (2006a). Dishevelled genes mediate a conserved mammalian PCP pathway to regulate convergent extension during neurulation. *Development* **133**, 1767-1778.
Wang, Y., Guo, N. and Nathans, J. (2006b). The role of Frizzled3 and Frizzled6 in neural tube closure and in the planar polarity of inner-ear sensory hair cells. *J. Neurosci.* **26**, 2147-2156.
Wang, S.-Z., Ibrahim, L. A., Kim, Y. J., Gibson, D. A., Leung, H. C., Yuan, W., Zhang, K. K., Tao, H. W., Ma, L. and Zhang, L. I. (2013). Slit/Robo signaling mediates spatial positioning of spiral ganglion neurons during development of cochlear innervation. *J. Neurosci.* **33**, 12242-12254.
Wang, Y., Williams, J., Rattner, A., Wu, S., Bassuk, A. G., Goffinet, A. M. and Nathans, J. (2016). Patterning of papillae on the mouse tongue: a system for the quantitative assessment of planar cell polarity signaling. *Dev. Biol.* **419**, 298-310.
Weisz, C., Glowatzki, E. and Fuchs, P. (2009). The postsynaptic function of type II cochlear afferents. *Nature* **461**, 1126-1129.
Yin, H., Copley, C. O., Goodrich, L. V. and Deans, M. R. (2012). Comparison of phenotypes between different vangl2 mutants demonstrates dominant effects of the Looptail mutation during hair cell development. *PLoS ONE* **7**, e31988.
Young, K. M., Mitsumori, T., Pringle, N., Grist, M., Kessaris, N. and Richardson, W. D. (2010). An Fgfr3-iCreER(T2) transgenic mouse line for studies of neural stem cells and astrocytes. *Glia* **58**, 943-953.
Zhou, L., Qu, Y., Tissir, F. and Goffinet, A. M. (2009). Role of the atypical cadherin Celsr3 during development of the internal capsule. *Cereb. Cortex* **19** Suppl. 1, i114-i119.